



King Fahd University of Petroleum & Minerals

DEPARTMENT OF MATHEMATICAL SCIENCES

Technical Report Series

TR 196

December 1995

**The Solution of the Riemann Problem for a Hyperbolic
System Modeling Polymer Flooding with Hysteresis**

Khaled M. Furati

THE SOLUTION OF THE RIEMANN PROBLEM FOR A HYPERBOLIC SYSTEM MODELING POLYMER FLOODING WITH HYSTERESIS

KHALED M. FURATI

Department of Mathematical Sciences

King Fahd University of Petroleum and Minerals

Dhahran 31261, Saudi Arabia

ABSTRACT. It is well-known that multi-phase flow in porous media exhibits hysteresis. This is typically modeled by modifying the saturation dependence of the relative permeabilities. In this paper, a model for hysteretic relative permeabilities is built into the polymer flooding model and the analytical solution to the corresponding Riemann problem is constructed. This produces a non-strictly hyperbolic system of conservation laws with a history-dependent flux function. Because the polymer model without hysteresis possesses Riemann problem solutions that are not monotonic, the introduction of hysteresis necessarily produces structurally different solutions. We show that hysteresis produces more complicated solutions with more fronts and expansions; and removes some non-uniqueness of solutions.

1. INTRODUCTION

In this paper we solve the Riemann problem for the system of conservation laws

$$\begin{aligned} \partial_t s + \partial_x F &= 0, \\ \partial_t(cs) + \partial_x(cF) &= 0, \end{aligned} \tag{1}$$

with the flux function F of the form

$$F = \begin{cases} f(s, c) & \text{if } s = \pi, \partial_t s > 0, \quad (\text{primary flow}) \\ h(s, \pi, c) & \text{otherwise,} \quad (\text{secondary flow}) \end{cases} \tag{2}$$

and initial conditions

$$(s, \pi, c)(x, 0) = \begin{cases} (s^L, \pi^L, c^L) & x \leq 0, \\ (s^R, \pi^R, c^R) & x > 0, \end{cases} \tag{3}$$

where, $t > 0$, $x \in \mathcal{R}$. The variables $s, \pi, c \in I$ and $s \leq \pi$, where I is the interval $[0, 1]$. The system (1) is used in enhanced oil recovery to model polymer flooding in which oil is displaced by water containing dissolved polymer. The variable s is the saturation of the aqueous phase and c is the concentration of polymer. The flux function F is the fractional flow function for the aqueous phase and π is the hysteresis parameter. For the derivation of (1) and physical assumptions see [12].

Experiments have shown that the flow functions are not only functions of current fluid saturations but also functions of the saturation history. Moreover, the solution of the Riemann problem for the polymer flooding model without hysteresis [5] shows cases with non-monotonic behavior in saturation. The form of F in (2) is based on remembering the saturation history through parameterizing the states at which the imbibition process is reversed. The function $F = f(s, c)$ describes the flow when the saturation increases monotonically from the irreducible aqueous phase saturation s_{ra} to the maximum saturation $1 - s_{rl}$, where s_{rl} is the residual liquid phase saturation. We will consider this imbibition of the aqueous phase as the *primary flow*. When this imbibition process is reversed at $s = \pi$, a new flow function $F = h(s, \pi, c)$ appears and the flow is called a *secondary flow*.

The main contribution of this paper is incorporating the flow history into the flux function and constructing the unique global solution of the Riemann problem. The Oleinik entropy condition [11] for scalar equations and the generalized Lax entropy condition [7] are used to distinguish the physically meaningful discontinuities. The solution is constructed by piecing together a compatible sequence of elementary waves (shocks, rarefactions, contact discontinuities) to connect constant states.

Including hysteresis produces more complicated solutions. Another effect of including hysteresis is that it removes some of the non-uniqueness cases arises in [5] where the solution is unique in the x, t -space but not in the state space. However, for some π^R large enough the same non-uniqueness problem persists. Although for certain critical values of the left and right states the solution is not pointwise continuous with respect to the left and right states, it is continuous in L^1 norm.

Buckley and Leverett [1] constructed the analytical solution for immiscible waterflooding. System (1) reduces to their single equation model when c is constant. Pope [12] generalized the fractional

flow theory to more complicated floodings and used the method of characteristics to construct the corresponding solutions. The polymer flooding model without hysteresis was analyzed and solved by Isaacson [5] and Johansen and Winther [6]. The problem is similar to the Riemann problem for vibration of an elastic string considered by Keyfitz and Kranzer [7].

Hysteresis phenomena in multi-phase flows in porous media has been recognized by many researchers. For example, Colonna et al. [2], Killough [8], Gladfelter and Gupta [4] and Lenhard [9]. Marchesin et al. [10] used a double-valued flux function to model two-phase flow with hysteresis and constructed, graphically, the complete solution of the associated Riemann problem. However, in this paper we consider a three-component two-phase flow with a more complicated model of hysteresis. The treatment of the history dependence in this paper is similar to that of motion in an elastic-plastic bar studied by Trangenstein and Pember in [13].

The outline of the paper is as follows. In Section 2 we present a brief derivation of the model. In Section 3 we state the mathematical assumptions and properties of the flux functions and analyze the hyperbolicity of the model. In Section 4 we discuss the different wave families. In Sections 5-8 we construct the Global solution for the Riemann problem.

2. DERIVATION OF THE MODEL

In polymer flooding, a solution of water and polymer is injected into an oil reservoir to push the oil through the rock. The reservoir fluid is considered to consist of three components: oil, water and polymer. The oil forms its own *liquid* phase, and water with polymer form the *aqueous* phase. The polymer transports only in the aqueous phase and does not partition to oil. The purpose of the polymer is to increase the viscosity of water, thereby enhancing its ability to push the oil.

System (1) is derived under many assumptions. We assume that the reservoir rock is homogeneous, so that the porosity and total permeability of the rock are constant. For the phases, we assume incompressibility and that the liquid phase viscosity is constant, but the aqueous phase viscosity increases as the concentration of polymer increases. Moreover, we assume that there are no diffusive forces, such as capillary pressure, and no gravity forces.

The mass conservation equations for water, oil and polymer, respectively, can be formulated as

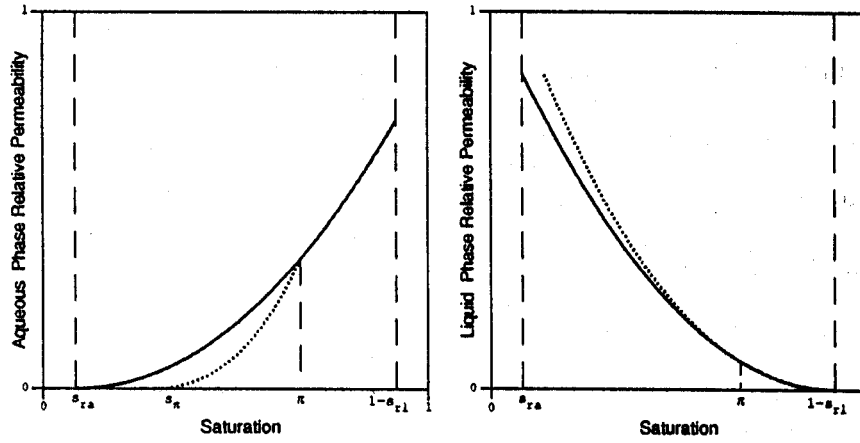


FIGURE 1. Hysteretic relative permeability curves.

follows:

$$\begin{aligned}\phi \partial_t s_a + \partial_x v_a &= 0, \\ \phi \partial_t s_l + \partial_x v_l &= 0, \\ \phi \partial_t (c s_a) + \partial_x (c v_a) &= 0,\end{aligned}\tag{4}$$

where ϕ is the rock porosity, c is the polymer concentration and s_a and s_l are the aqueous and liquid phases saturations, respectively. The fluxes v_a and v_l are the volumetric flow rates of the aqueous and liquid phases, respectively, and are given by Darcy's law:

$$v_a = -\frac{K k_{ra}}{\mu_a(c)} \partial_x P, \quad v_l = -\frac{K k_{rl}}{\mu_l} \partial_x P.\tag{5}$$

Here, P is the fluid pressure, K is the absolute permeability of the rock, k_{ra} and k_{rl} are the relative permeabilities of the aqueous and liquid phases, respectively, and μ_a , μ_l are the corresponding viscosities.

Next, we use the assumption that the total velocity $v_t = v_a + v_l$ is constant to eliminate the pressure gradient. Adding the first two equations in (4), using the assumption that $s_l + s_a = 1$ and changing x to $\phi x/v_t$ we obtain (1) with $s = s_a$ and

$$F = \frac{k_{ra}}{k_{ra} + k_{rl} \mu(c)},\tag{6}$$

where $\mu = \mu_a/\mu_l$ is the viscosity ratio.

To complete the description of the conservation laws we need to describe the relative permeability curves. In this paper, we will consider the typical relative permeability curves shown in Figure 1, with the aqueous phase being the wetting phase. The solid curves give the relative permeability

values when the saturation s is monotonically increasing from s_{ra} . We will call such curves the *primary* curves. When the aqueous phase saturation decreases, the relative permeability will be smaller and follow the dashed curves. We will call such curves the *secondary* curves. When the saturation increases again, we will assume that the relative permeability will trace back the secondary curve until it meets the primary curve, then will follow the primary curve.

We will parameterize the secondary curves by the symbol π , which we will refer to as the hysteresis parameter. The primary and secondary curves are denoted by $k_{rj}(s)$ and $k_{rj}^h(s, \pi)$, respectively, where $j = a, l$. Thus we have

$$k_{rj} = \begin{cases} k_{rj}(s) & \text{if } s = \pi, \partial_t s > 0, \\ k_{rj}^h(s, \pi) & \text{otherwise,} \end{cases} \quad j = a, l. \quad (7)$$

With the above forms of the relative permeability curves, the fractional flow function F takes the form (2) with

$$f(s, c) = \frac{k_{ra}(s)}{k_{ra}(s) + k_{rl}(s) \mu(c)}, \quad h(s, \pi, c) = \frac{k_{ra}^h(s, \pi)}{k_{ra}^h(s, \pi) + k_{rl}^h(s, \pi) \mu(c)}. \quad (8)$$

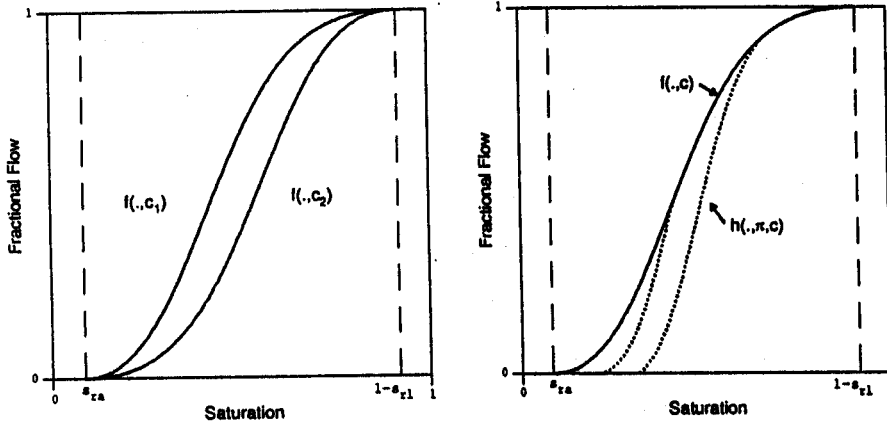
Figure 2 shows typical fractional flow curves.

Note that since the polymer will increase water viscosity, the ratio $\mu = \mu(c)$ is an increasing function of c . This implies that the fractional flow function F is decreasing with respect to c . Physically, this means that adding polymer will increase the oil flow rate which is equal to $1 - F$.

3. THE MATHEMATICAL DESCRIPTION OF THE MODEL

In this section we present the mathematical assumptions and properties of the relative permeabilities and hence the flux functions. Accordingly, we will analyze the hyperbolicity of the system of conservation laws (1). Let $I = [0, 1]$, $I_s = [s_{ra}, 1 - s_{rl}]$ and $I_\pi = [s_\pi, \pi]$, where $s_\pi = \max\{s : h(s, \pi, c) = 0\}$. We will assume that the relative permeability curves satisfy the following conditions, as shown in Figure 1:

- A1. $k_{rj}(s) \in C^2(I_s)$, $k_{rj}^h(s, \pi) \in C^2(I_\pi)$ in s and $\in C^1(I_s)$ in π , where $j = a, l$;
- A2. $k_{rj}^h(s, s) = k_{rj}(s)$, $\forall s \in I_s$, $j = a, l$;
- A3. $k'_{ra} > 0$, $k''_{ra} > 0$, $k'_{rl} < 0$ and $k''_{rl} > 0$, $\forall s \in I_s$;

FIGURE 2. Fractional flow curves, $c_2 > c_1$.

A4. $\partial_s k_{ra}^h > 0$, $\partial_\pi k_{ra}^h < 0$, $\partial_{ss} k_{ra}^h > 0$, $\partial_s k_{rl}^h < 0$, $\partial_\pi k_{rl}^h > 0$ and $\partial_{ss} k_{rl}^h > 0$ in $I_\pi \times I_s$;

A5. $k'_{ra}(s_{ra}) + \mu(c) k'_{rl}(s_{ra}) \leq 0$ and $k'_{ra}(1 - s_{rl}) + \mu(c) k'_{rl}(1 - s_{rl}) \geq 0$, $\forall c \in I$;

A6. $\partial_s k_{ra}^h(s_\pi, \pi) + \mu(c) \partial_s k_{rl}^h(s_\pi, \pi) \leq 0$, $\forall c \in I$.

Assumption A5 is a sufficient (not necessary) condition for the primary fractional flow function, $f(., c)$, to be convex in a neighborhood of $s = s_{ra}$ and concave in a neighborhood of $s = 1 - s_{rl}$.

This implies the existence of an inflection point of f .

We assumed $\partial_\pi k_{ra}^h < 0$ and $\partial_\pi k_{rl}^h > 0$ so that the secondary relative permeability curves are disjoint for distinct values of π . Assumption A6 is a sufficient (not necessary) condition for the secondary fractional flow function $h(s, \pi, c)$ to be convex in some neighborhood of the irreducible saturation s_π .

With direct examinations of the derivatives, the above assumptions imply the following properties for the flux functions f and h as shown in Figure 2.

P1. $f(s, c)$ is a C^2 function in $I_s \times I$, and $f(s_{ra}, c) = 0$ and $f(1 - s_{rl}, c) = 1$, $\forall c \in I$;

P2. $\partial_s f(s, c) > 0$ and $\partial_c f(s, c) < 0$ in $I_s \times I$;

P3. For each $c \in I$, there is an inflection point, $s^I = s^I(c) \in (s_{ra}, 1 - s_{rl})$, such that $\partial_{ss} f(s, c) > 0$ for $s < s^I$;

P4. $h(s, \pi, c)$ is a C^2 function in $s \in I_\pi$, C^1 in $\pi \in I_s$ and C^2 in $c \in I$;

P5. $h(s_\pi, \pi, c) = 0$ and $h(s, s, c) = f(s, c)$ for each $\pi, s \in I_s$ and $c \in I$;

P6. $\partial_s h(s, \pi, c) > 0$, $\partial_\pi h(s, \pi, c) < 0$ and $\partial_c h(s, \pi, c) < 0$ in $I_\pi \times I_s \times I$;

P7. $\partial_{ss}h(s_\pi, \pi, c) > 0$, for each $c \in I$ and $\pi \in I_s$, and h has at most one inflection point $s^I(\pi, c)$, for $s \in I_\pi$;

P8. $\partial_s f(\pi, c) \leq \partial_s^- h(\pi, \pi, c)$, for each $c \in I$, where ∂_s^- is the left derivative.

Note that the assumptions on relative permeability curves imply existence (property P3) but not necessarily uniqueness of the inflection points of f . However, for most applications, experimental data indicates that the fractional flow function does not have more than one inflection point. Therefore, for each $c \in I$ we will assume that $s^I(c)$ is the only point of inflection, and consequently, $f(., c)$ is convex in $(s_{ra}, s^I(c))$ and concave in $(s^I(c), 1 - s_{rl})$.

Property P6 implies that the secondary fractional flow curves for a fixed c are disjoint for distinct values of π . Also, it implies that for a fixed π the curves are disjoint for distinct values of c .

Unlike the primary fractional flow function, $f(s, c)$, assumptions on $k_{ra}^h(s, \pi)$ and $k_{rl}^h(s, \pi)$ do not guarantee the existence of inflection points for the secondary fractional flow function, h . Moreover, the assumptions do not guarantee the uniqueness of such points for the curves of h , as for f . The assumptions only guarantee Property P7 which implies that all the curves of h are convex in some neighborhood of s_π . We will assume that for each $c \in I$ and $\pi \in I_s$, $h(s, \pi, c)$ has at most one inflection point, $s^I(\pi, c)$, for $s \in I_\pi$.

For the primary flow, system (1) can be written in the quasilinear form

$$\partial_t \begin{bmatrix} s \\ c \end{bmatrix} + A \partial_x \begin{bmatrix} s \\ c \end{bmatrix} = 0, \quad A = \begin{bmatrix} \partial_s f & \partial_c f \\ 0 & f/s \end{bmatrix}. \quad (9)$$

Since the eigenvalues of A are real, the system of conservation laws is hyperbolic, and has the two characteristic speeds and the corresponding eigenvectors:

$$\lambda_b = \partial_s f, \quad r_b = \begin{bmatrix} 1 \\ 0 \end{bmatrix}, \quad \lambda_p = \frac{f}{s}, \quad r_p = \begin{bmatrix} \partial_c f \\ \lambda_p - \lambda_b \end{bmatrix}. \quad (10)$$

The characteristic speed λ_b is the Buckley-Leverett rarefaction wave speed, which is equal to the slope of f . The second characteristic speed, λ_p , is the aqueous particle velocity, which is equal to the slope of the chord from the origin to the fractional flow function.

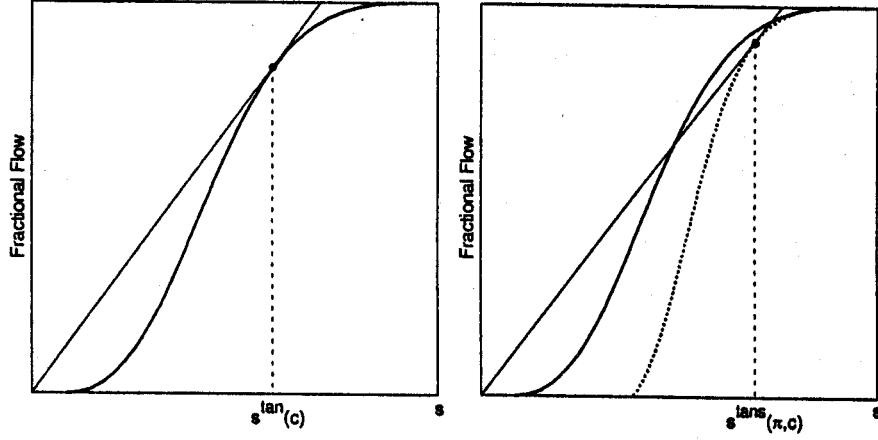


FIGURE 3. Tangential states.

If the flow is secondary, $F = h(s, \pi, c)$, then the system of conservation laws (1) can be closed by adding the constraint $\partial_t \pi = 0$ and written in the quasilinear form

$$\partial_t \begin{bmatrix} s \\ c \\ \pi \end{bmatrix} + \tilde{A} \partial_x \begin{bmatrix} s \\ c \\ \pi \end{bmatrix} = 0, \quad \tilde{A} = \begin{bmatrix} \partial_s h & \partial_c h & \partial_\pi h \\ 0 & h/s & 0 \\ 0 & 0 & 0 \end{bmatrix}. \quad (11)$$

The characteristic speeds and their corresponding eigenvectors are

$$\lambda_{bs} = \partial_s h, \quad r_{bs} = \begin{bmatrix} 1 \\ 0 \\ 0 \end{bmatrix}, \quad \lambda_{ps} = \frac{h}{s}, \quad r_{ps} = \begin{bmatrix} \partial_c h \\ \lambda_{ps} - \lambda_{bs} \\ 0 \end{bmatrix}, \quad \lambda_\pi = 0, \quad r_\pi = \begin{bmatrix} \partial_\pi h \\ 0 \\ -\lambda_{bs} \end{bmatrix} \quad (12)$$

Note that all the characteristic speeds are non-negative. This implies that all the wave families are either stationary or traveling to the right.

For the border states $u = (\pi, \pi, c)$, we define the Buckley-Leverett characteristic speeds by: $\lambda_b(\pi, \pi, c) = \partial_s f(\pi, c)$ and $\lambda_{bs}(\pi, \pi, c) = \partial_s^- h(\pi, \pi, c)$. The type of the flow (secondary or primary) determines which velocity is to be used in determining the Riemann problem solutions.

Note that for a given c the Buckley-Leverett and particle velocities might coalesce as shown in Figure 3. However, this is not always the case as shown in Figure 4. We let $u^{tan}(c)$ and $u^{tan}(\pi, c)$ be the states such that $\lambda_b(u^{tan}) = \lambda_p(u^{tan})$ and $\lambda_{bs}(u^{tan}) = \lambda_{ps}(u^{tan})$. For the fractional flow curves described above we have the following results.

Lemma 3.1. *For each $c \in I$, $f(\cdot, c)$ has at most one tangential state $u^{tan}(c)$. If such a state exists, then $\lambda_b(s, c) > \lambda_p(s, c)$ for $s_{ra} < s < s^{tan}(c)$ and $\lambda_b(s, c) < \lambda_p(s, c)$ for $s^{tan}(c) < s$.*

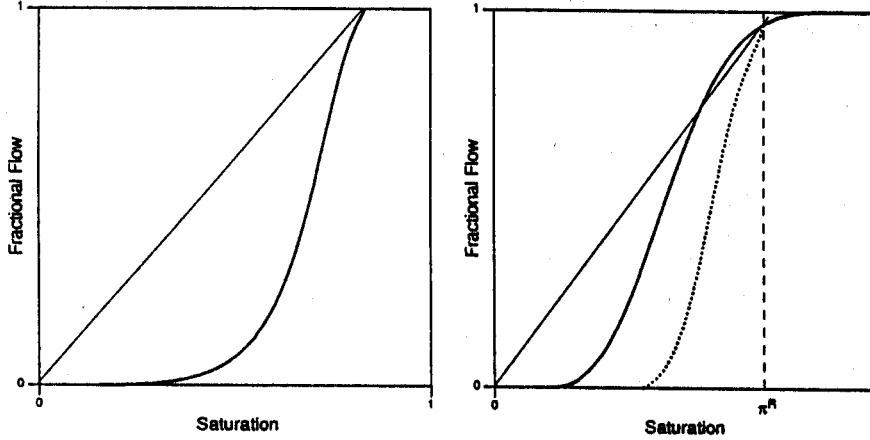


FIGURE 4. No tangential states.

Proof. Note that by definition, the tangential states u^{tan} are the solutions of the equation $\lambda_b - \lambda_p = \partial_s f - f/s = 0$. Given $c \in I$, let $g(s) = s \partial_s f(s, c) - f(s, c)$, for $s \in (s_{ra}, 1 - s_{rl})$. Since $g'(s) = s \partial_{ss} f(s, c)$ and $f(s, c)$ is assumed to have a unique inflection point $u^I = (s^I(c), c)$, $g(s)$ has only one local maximum at s^I in $(s_{ra}, 1 - s_{rl})$. Therefore, $g = 0$ can have at most one solution since $g(s_{ra}) \geq 0$. This proves the uniqueness because any s^{tan} is by definition a solution of $g = 0$. The second part follows from the observation that g changes from positive to negative at $s = s^{tan}$. \square

The next lemma shows for which values of π the tangential state u^{tans} might exist.

Lemma 3.2. For a given $c \in I$ and $\pi < s^{tan}(c)$, $\lambda_{bs}(s, \pi, c) > \lambda_{ps}(s, \pi, c)$ for $s \in (s_\pi, \pi]$.

Proof. For a fixed $c \in I$ and $\pi \in (s_{ra}, s^{tan}(c))$, let $g(s) = s \partial_s h(s, \pi, c) - h(s, \pi, c)$. From Property P7 of the secondary fractional flow curves, we have $g'(s_\pi) = s_\pi \partial_{ss} h(s_\pi, \pi, c) > 0$. In addition, g satisfies the following inequalities:

$$\begin{aligned} g(s_\pi) &= s_\pi \partial_s h(s_\pi, \pi, c) \geq 0, \\ g(\pi) &= \pi \partial_s^- h(\pi, \pi, c) - h(\pi, \pi, c) > \pi \partial_s f(\pi, c) - f(\pi, c) > 0. \end{aligned} \quad (13)$$

From those inequalities and the assumption that h has at most one inflection state, it follows that g is positive for $s \in (s_\pi, \pi]$. This proves the result. \square

The above lemma implies that the tangential state, $u^{tans} = (s^{tans}(\pi, c), \pi, c)$, may only exist if $\pi \geq s^{tan}(c)$. The following lemma is about the uniqueness of u^{tans} .

Lemma 3.3. Given $c \in I$ and $\pi \geq s^{tan}(c)$, there exists at most one tangential state $u^{tans}(\pi, c) = (s^{tans}(\pi, c), \pi, c)$, $s_{ra} < s^{tans} < \pi$.

Proof. As in the proof of Lemma 3.1, the result follows from the uniqueness of the inflection point of h . \square

In the above proofs, note that the uniqueness of the tangential states follows from the uniqueness of the inflection points. However, this does not guarantee their existence. In this paper we will assume the existence of u^{tan} but not necessarily u^{tans} . However, if for $\pi \geq s^{tan}$ the state u^{tans} does not exist we have the following lemma.

Lemma 3.4. *Given $c \in I$ and $\pi \geq s^{tan}(c)$, if there is no tangential state u^{tans} , then the state $u^\pi = (\pi, \pi, c)$ satisfies*

$$[\lambda_{bs}(u^\pi) - \lambda_{ps}(u^\pi)][\lambda_b(u^\pi) - \lambda_p(u^\pi)] \leq 0. \quad (14)$$

Proof. Again, for fixed c and π consider the function $g(s) = s \partial_s h - h$. By assumption, $g = 0$ has no solution for $s \in (s_\pi, \pi)$. But $g(s_\pi) \geq 0$ and $g'(s_\pi) > 0$. Therefore, $g(s) > 0$ for $s_\pi < s < \pi$. By continuity, this implies that $g(\pi) \geq 0$, and thus the first bracket in the inequality (14) is non-negative. The second bracket is non-positive by Lemma 3.1. This proves the result. \square

To summarize, for each $c \in I$ we assume that there exists a state $u^{tan} = (s^{tan}(c), c)$ such that $\lambda_p(u^{tan}) = \lambda_b(u^{tan})$. Moreover, for each $c \in I$ and $\pi \in I_s$, if $\pi < s^{tan}(c)$ then $\lambda_{ps}(u) < \lambda_{bs}(u)$ for all $u = (s, \pi, c)$ with $s_\pi < s \leq \pi$. If $\pi \geq s^{tan}(c)$, then either there exists a state $u^{tans} = (s^{tans}(\pi, c), \pi, c)$ such that $\lambda_{ps}(u^{tans}) = \lambda_{bs}(u^{tans})$ or the state (π, π, c) is a transitional state across which the relation between the two speeds is reversed. Both states u^{tan} and u^{tans} are unique.

We will partition the set of all states into the following sets:

$$\begin{aligned} \mathcal{P} &= \{u : \lambda_p(u) > \lambda_b(u)\}, & \mathcal{B} &= \{u : \lambda_b(u) > \lambda_p(u)\}, & \mathcal{T} &= \{u : \lambda_p(u) = \lambda_b(u)\}, \\ \mathcal{P}_s &= \{u : \lambda_{ps}(u) > \lambda_{bs}(u)\}, & \mathcal{B}_s &= \{u : \lambda_{bs}(u) > \lambda_{ps}(u)\}, & \mathcal{T}_s &= \{u : \lambda_{ps}(u) = \lambda_{bs}(u)\}. \end{aligned}$$

Those sets will be used in characterizing the different cases for the solutions.

4. WAVE FAMILIES

In this section we will determine all wave families associated with the Riemann problem (1)–(3). Those wave families consist of the elementary waves: rarefactions, shocks and contact discontinuities.

To find all the possible waves we need to examine the nonlinearity of the characteristic fields, the conditions for discontinuities and the integral curves of the characteristic eigenvectors.

For the nonlinearity we need to check the projection of the characteristic speed gradient into the corresponding eigenvector. For our problem we have

$$\nabla \lambda_p \cdot r_p = \nabla_\pi \lambda_{ps} \cdot r_{ps} = \nabla_\pi \lambda_\pi \cdot r_\pi = 0, \quad \nabla \lambda_b \cdot r_b = \partial_{ss} f, \quad \nabla_\pi \lambda_{bs} \cdot r_{bs} = \partial_{ss} h,$$

where $\nabla = (\partial_s, \partial_c)$ and $\nabla_\pi = (\partial_s, \partial_c, \partial_\pi)$. Consequently, the p -field, ps -field and π -field are linearly degenerate and therefore the corresponding families consist only of contact discontinuities. On the other hand, due to the inflection points of f and h , the b -family and bs -family are not typically genuinely nonlinear. We expect both families to consist of rarefactions and shocks.

As we know, any discontinuity solution of speed σ must satisfy the Rankine-Hugoniot conditions.

For the primary flow those conditions take the form

$$\begin{bmatrix} f^R - f^L \\ c^R f^R - c^L f^L \end{bmatrix} = \begin{bmatrix} s^R - s^L \\ c^R s^R - c^L s^L \end{bmatrix} \sigma. \quad (15)$$

One solution for (15) is $\sigma = \lambda_p = f/s$. Another solution is determined by taking c to be constant and $\sigma = [f]/[s]$, where $[.]$ denotes the jump of the argument across the discontinuity.

For the secondary flow, the Rankine-Hugoniot conditions take the form

$$\begin{bmatrix} h^R - h^L \\ c^R h^R - c^L h^L \\ 0 \end{bmatrix} = \begin{bmatrix} s^R - s^L \\ c^R s^R - c^L s^L \\ \pi^R - \pi^L \end{bmatrix} \sigma. \quad (16)$$

The conditions in (16) have the three solutions:

- (1) $\sigma = [h]/[s]$ and $[c] = [\pi] = 0$;
- (2) $\sigma = \lambda_{ps} = h/s$ and $[\pi] = 0$;
- (3) $\sigma = 0$ and $[h] = [c] = 0$.

To search for rarefactions we need to consider the integral curves of the eigenvectors r_b and r_{bs} . The integral curves of r_b are the curves where c is constant. Similarly, the integral curves of r_{bs} are the curves where c and π are constant.

Accordingly, the wave families for the Riemann problem for system (1)–(3) can be classified as follows.

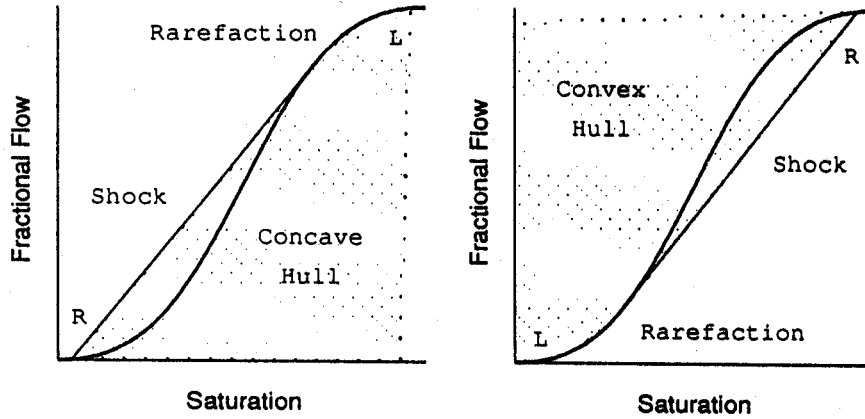


FIGURE 5. Concave and convex hulls.

b -waves and bs -waves. The two families correspond to the characteristic speeds λ_b and λ_{bs} , respectively, and consist of rarefactions and shocks. Note that c is a Riemann invariant of both families and π is a Riemann invariant of the bs -family. Thus, from the solutions of the Rankine-Hugoniot conditions, the wave curves for the shocks and rarefactions of both families are identical. The b -family curves are the ones along which c is constant. The bs -family curves are the ones along which both c and π are constants. As a result, both families can be considered as solutions of the scalar equation $\partial_t s + \partial_x F = 0$, $F = f, h$.

To distinguish the physically meaningful shocks, we need to impose an entropy condition. For our purpose, a shock is considered admissible if it satisfies the Oleinik condition [11] for scalar equations. This condition requires that

$$\frac{F(u^R) - F(u)}{s^R - s} \leq \sigma = \frac{F(u^R) - F(u^L)}{s^R - s^L} \quad (17)$$

for all s between s^L and s^R . In other words, the chord from $(s^R, F(u^R))$ to $(s^L, F(u^L))$ must lie above the chord from $(s^R, F(u^R))$ to $(s, F(u))$ for any s in between.

Since both families are not genuinely nonlinear, the solution may consist of a combination of a shock and rarefaction. For the rarefactions, the characteristic speeds should be monotonically increasing from left to right. This monotonicity and Oleinik condition are equivalent to constructing the concave hull for $s^L > s^R$ and the convex hull for $s^L < s^R$ as shown in Figure 5. A straight line segment represents a shock and a curve segment represents a rarefaction. The shock speed is equal to the slope of the straight line.

In petroleum engineering literature, the above solutions are usually explained in terms of Welge

tangents [3, 14]. The Welge tangents are equivalent to the Oleinik chords for such problems.

We will use k -wave, $k = b, bs$, to denote a k -shock, k -rarefaction or any consecutive combination of them. Note that to have a b -wave we must have $s^L > s^R$ so it corresponds to a primary flow.

p -waves and ps -waves. The two families correspond to the characteristic speed λ_p and λ_{ps} , respectively. The two families are linearly degenerate and consist of contact discontinuities since λ_p and λ_{ps} are Riemann invariants.

The wave curves for the p -family are the curves $c = c(s)$ along which λ_p is constant. The slope of such curves depends on the relation between λ_p and λ_b since $dc/ds = (\lambda_p - \lambda_b)/f_c$. The same argument is true for the ps -family curves $c = c(s, \pi)$.

The states $u^L = (s^L, c^L)$ and $u^R = (s^R, c^R)$, $s^L > s^R$, can be connected by a contact discontinuity if $\lambda_p(u^L) = \lambda_p(u^R)$ and they both belong to either $\mathcal{P} \cup \mathcal{T}$ or $\mathcal{B} \cup \mathcal{T}$. The last condition is to fulfill the generalized Lax's entropy condition [7] which requires that exactly one of the b -characteristics leave the discontinuity. With $\pi^L = \pi^R$, similar results are true for the ps -family.

st -waves. This family consists of stationary contact discontinuities satisfying Rankine-Hugoniot conditions with speed $\sigma = 0$. Across this discontinuity, $[h] = [c] = 0$.

5. GLOBAL SOLUTION OF THE RIEMANN PROBLEM

The global solution to the Riemann problem can be constructed graphically using the wave families mentioned above. The uniqueness of the solutions can easily be verified by imposing the compatibility condition, i.e. the initial speed of each wave is greater than or equal to the final speed of the preceding wave. We will start with the following remarks.

Remark 1 (Notation). Although the problem during a primary flow is independent of the history parameter π , we will write any state $u = (s, c)$ as $u = (s, s, c)$. Thus, for primary and secondary flows we can let $u^L = (s^L, \pi^L, c^L)$ and $u^R = (s^R, \pi^R, c^R)$ be the left and right states of the Riemann problem. For the rest of this paper we will use $h(s, s, c)$ to denote $f(s, c)$. For simplicity, we will use h^α to denote $h(u^\alpha)$ and λ^α to denote $\lambda(u^\alpha)$. Moreover, we will use \xrightarrow{k} to denote a k -wave.

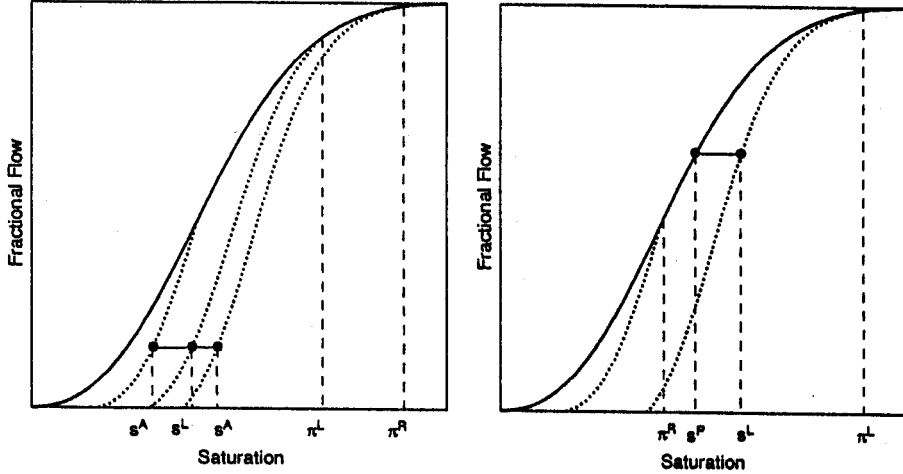


FIGURE 6. Left: $h^Q \geq h^L$. Right: $h^Q < h^L$.

Remark 2 (Reduction). For any given two states $u^L = (s^L, \pi^L, c^L)$ and $u^R = (s^R, \pi^R, c^R)$ let $u^Q = (\pi^R, \pi^R, c^L)$. Accordingly, there are two cases as shown in Figure 6. If $h^Q \geq h^L$, then there is a unique state $u^A = (s^A, \pi^R, c^L)$ such that $h^A = h^L$, and u^L can be connected to u^A by a stationary wave $u^L \xrightarrow{st} u^A$. Otherwise, there is a unique state $u^P = (s^P, s^P, c^L)$, $s^P \leq s^L$, such that $h^P = h^L$ and u^L can be connected to u^P by a stationary wave $u^L \xrightarrow{st} u^P$. Thus, the problem can be reduced to solving either for $u^L = (s^L, \pi^R, c^L)$ or $u^L = (s^L, s^L, c^L)$, $\pi^R < s^L$, for any arbitrary u^R .

To account for all possible cases, we will treat three different cases separately: $c^L = c^R$, $c^L > c^R$ and $c^L < c^R$. Solutions of the Riemann problem will be composed of compatible sequences of the st -waves, bs -waves, b -waves, p -waves and ps -waves.

6. THE CASE $c^L = c^R$ (BUCKLEY-LEVERETT EQUATION WITH HYSTERESIS)

When $c^L = c^R$, the system (1) degenerates to the Buckley-Leverett equation and the solution will consist of b -waves and bs -waves. For this special case we will omit the concentration argument and write any state u as $u = (s, \pi)$. From Remark 2, we only need to consider the following two cases.

1. $u^L = (s^L, \pi^R)$. In this case, u^L and u^R lie on the same secondary curve $h = h(s, \pi^R)$. The solution is a bs -wave determined by the concave hull if $s^R < s^L$ or by the convex hull if $s^R > s^L$. Thus, we have the wave $u^L \xrightarrow{bs} u^R$ across which π is constant and is equal to π^R . See Figure 7 for the case $s^R < s^L$.

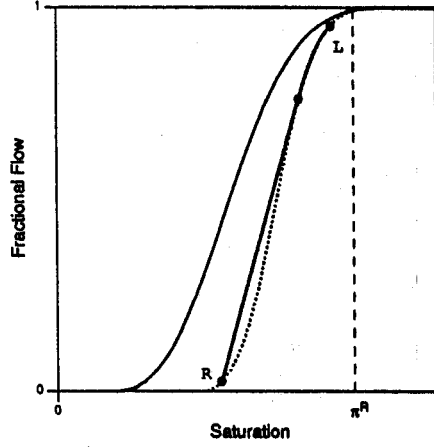


FIGURE 7. Solution for $c^L = c^R$, $\pi^L = \pi^R$ and $s^L > s^R$.

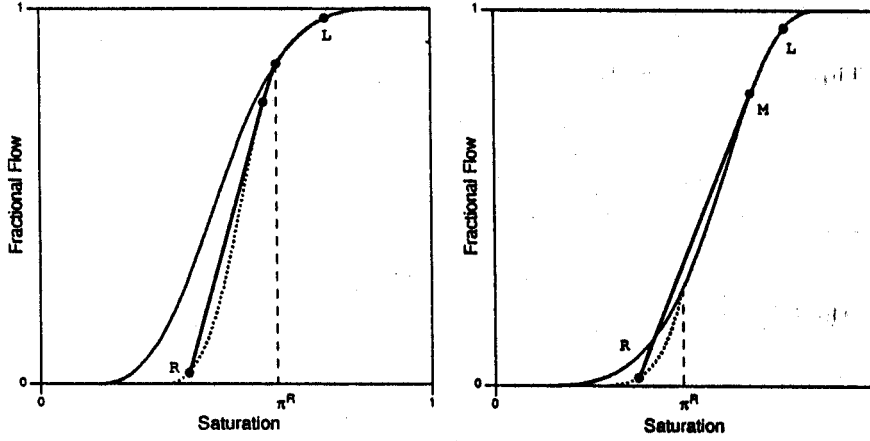


FIGURE 8. Solutions for $c^L = c^R$ and $s^L = \pi^L > \pi^R$.

2. $u^L = u(s^L, s^L)$ and $\pi^R < s^L$. Consider first the intermediate states $u = (s, s)$, $\pi^R \leq s < s^L$. The left state u^L can be connected to any of those states by a unique b -wave determined by the concave hull of the primary curve joining the two states. In particular, for the state (π^R, π^R) we have the connection $u^L \xrightarrow{b} (\pi^R, \pi^R)$. On the other hand, the state (π^R, π^R) can be connected to the right state u^R by a unique bs -wave determined by the concave hull of the secondary curve. Thus, we have $(\pi^R, \pi^R) \xrightarrow{bs} u^R$. If the final speed of the b -wave is less than the initial speed of the bs -wave, then the two waves are compatible and can be composed to give the unique solution $u^L \xrightarrow{b} (\pi^R, \pi^R) \xrightarrow{bs} u^R$ as shown in Figure 8a. Note that, in this case, the union of the two concave hulls is also concave. Otherwise, we need to construct the concave hull of the union of the two hulls as in Figure 8b. The saturation s^M satisfies

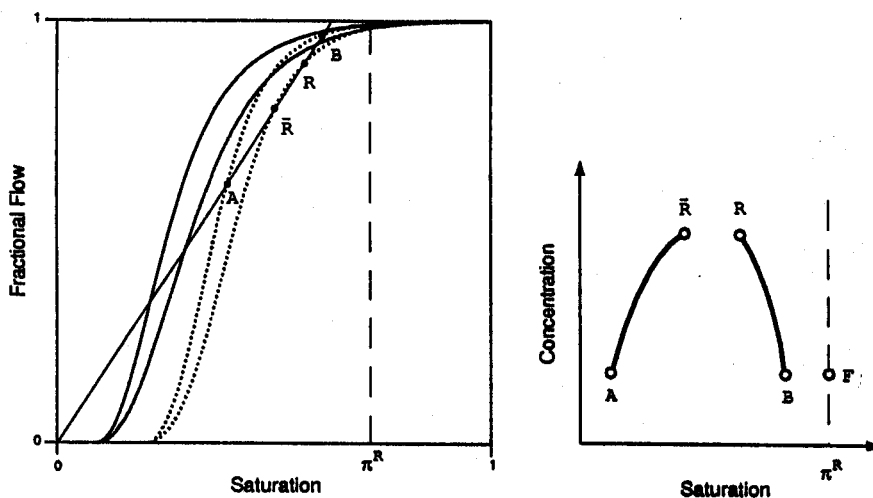
$$f'(s^M) = \frac{f(s^M) - h(s^R, \pi^R)}{s^M - s^R}. \quad (18)$$

$u^L \in \mathcal{B}_s \cup \mathcal{T}_s$	$u^R \in \mathcal{P}_s \cup \mathcal{T}_s$ and $\lambda_{ps}^R \leq \lambda_{ps}^L$ $u^L \xrightarrow{bs} u^I \xrightarrow{ps} u^R$	$\exists! u^I = (s^I, \pi^R, c^L) \in \mathcal{P}_s \cup \mathcal{T}_s \ni \lambda_{ps}^I = \lambda_{ps}^R.$	
	$u^R \in \mathcal{B}_s \cup \mathcal{T}_s$ or $\lambda_{ps}^R \geq \lambda_{ps}^L$ $u^L \xrightarrow{ps} u^I \xrightarrow{bs} u^R$	$\exists! u^I = (s^I, \pi^R, c^R) \in \mathcal{B}_s \ni \lambda_{ps}^I = \lambda_{ps}^L.$	
$u^L \in \mathcal{P}_s$	$\exists! u^T = (s^T, \pi^R, c^L) \in \mathcal{T}_s$ as in Figure 3.		
	$u^R \in \mathcal{P}_s \cup \mathcal{T}_s$ and $\lambda_{ps}^R \leq \lambda_{ps}^T$ $u^L \xrightarrow{bs} u^I \xrightarrow{ps} u^R$	$\exists! u^I = (s^I, \pi^R, c^L) \in \mathcal{P}_s \cup \mathcal{T}_s \ni \lambda_{ps}^I = \lambda_{ps}^R.$	
	$u^R \in \mathcal{B}_s \cup \mathcal{T}_s$ or $\lambda_{ps}^R \geq \lambda_{ps}^T$ $u^L \xrightarrow{bs} u^T \xrightarrow{ps} u^I \xrightarrow{bs} u^R$	$\exists! u^I = (s^I, \pi^R, c^R) \in \mathcal{B}_s \ni \lambda_{ps}^I = \lambda_{ps}^T.$	

TABLE I. Solutions for $c^L > c^R$ and $\pi^L = \pi^R$.

The intermediate states are as in Figure 9.			
$u^L \in BUT$	$\lambda_p^L \geq \lambda_p^F$	$u^L \xrightarrow{p} u^B \xrightarrow{b} u^F \xrightarrow{bs}$ u^R	
	$\lambda_p^L < \lambda_p^F$	$u^L \xrightarrow{p} u^I \xrightarrow{ps} u^J \xrightarrow{bs}$ u^R	
Let $u^T = (s^T, s^T, c^L) \in \mathcal{T}$.			
$u^L \in \mathcal{P}$	$s^T \leq \pi^R$	$u^A = (\pi^R, \pi^R, c^L).$ $u^L \xrightarrow{b} u^A \xrightarrow{\text{Section 7.1}} u^R$	
	$s^T > \pi^R$	$\lambda_p^T \geq \lambda_p^F$ $u^L \xrightarrow{b} u^T \xrightarrow{p} u^B \xrightarrow{b}$ $u^F \xrightarrow{bs} u^R$	
	$s^T > \pi^R$	$\lambda_p^T < \lambda_p^F$ $u^L \xrightarrow{b} u^T \xrightarrow{p} u^I \xrightarrow{ps}$ $u^J \xrightarrow{bs} u^R$	

TABLE II. Solutions for $c^L > c^R$ and $s^L = \pi^L > \pi^R$.


 FIGURE 10. The states u^A and u^B .

Case 2: $u^L \in \mathcal{P}$. The slowest wave that leaves u^L is a b -wave. How far this wave can be extended depends on the position of $u^T = (s^T, s^T, c^L) \in \mathcal{T}$ with respect to u^R .

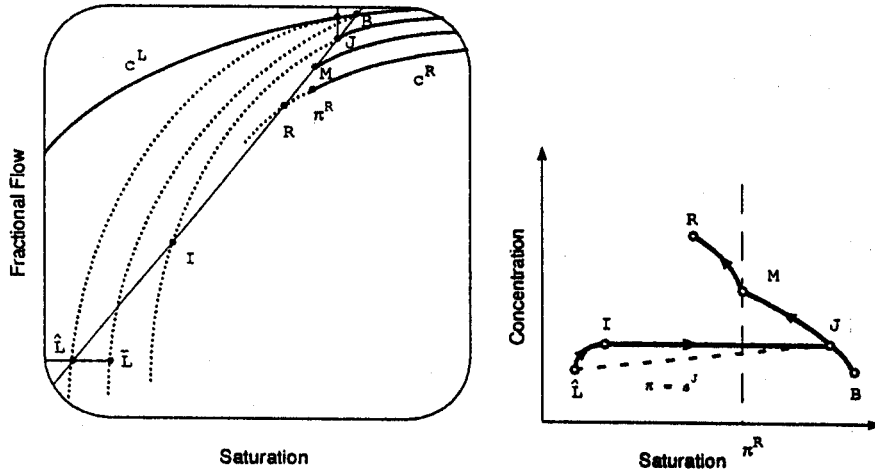
If $s^T \leq \pi^R$, then both u^L and $u^A = (\pi^R, \pi^R, c^L)$ lie on the concave part of the primary curve and can be connected by the rarefaction $u^L \xrightarrow{b} u^A$ with final speed equal to λ_b^A . Afterwards, u^A can be connected to u^R as in section 7.1. There, the wave that leaves u^A is either a bs -rarefaction or a ps -wave. The initial speed of both waves is greater than or equal to λ_b^A . Thus, the whole connection is compatible.

When $s^T > \pi^R$, u^T considered as the left state, can be connected to u^R as in Case 1 in which the initial speed of the p -wave leaving u^T is equal to λ_p^T . Moreover, u^L and u^T can be connected through a b -rarefaction. From the definition of u^T , the two waves are compatible.

8. THE CASE $c^L < c^R$

Considering the characteristic speeds at the right state, we treat the following two situations separately.

8.1. The Case $u^R \in \mathcal{P}_s \cup \mathcal{T}_s$. As shown in Figure 10, for a given c^L , the state u^R determines uniquely different states of the same particle velocity. The first one is the state $u^A = (s^A, \pi^R, c^L)$ such that $\lambda_{ps}^A = \lambda_{ps}^R$ and $u^A \in \mathcal{B}_s$. If $\lambda_{ps}^R \geq \lambda_{ps}^F$, where $u^F = (\pi^R, \pi^R, c^L)$, then there exists a state $u^B = (s^B, \pi^R, c^L) \in \mathcal{P}_s$ such that $\lambda_{ps}^B = \lambda_{ps}^R$. Otherwise, there exist the two states $u^M = (\pi^R, \pi^R, c^M) \in \mathcal{P}$, $c^L < c^M < c^R$, and $u^B = (s^B, s^B, c^L) \in \mathcal{P}$, $s^B > \pi^R$, such that $\lambda_p^M = \lambda_p^B = \lambda_{ps}^R$.

FIGURE 11. The cd -wave.

as in Figure 11.

If $\lambda_{ps}^R < \lambda_{ps}^F$, consider the case shown in Figure 11. In that case, we consider a left state $u^L = (s^L, \pi^L, c^L)$ such that $\lambda_{ps}^L > \lambda_{ps}^R$ and either $\pi^L = \pi^R$ or $s^L = \pi^L > \pi^R$. Let $u^L = (s^L, s^B, c^L)$ be the state such that $h^L = h^L$. Thus, u^L can be connected to u^L by a stationary contact discontinuity and to u^B by a bs -wave along the convex hull with constant $\pi = s^B$. Since u^B lies on a concave segment, the bs -wave will end with a shock. To have a compatible sequence, we must have the shock speed less than or equal to λ_p^B . By inspecting the convex hull joining u^L and u^B , this is equivalent to the condition that $\lambda_{ps}^L \geq \lambda_{ps}^R$ and the bs -wave is necessarily a shock. However, when $\lambda_{ps}^L < \lambda_{ps}^R$, the final speed of the wave $u^L \xrightarrow{bs} u^B$ is greater than λ_p^B and the above sequence is incompatible. Figure 11 suggests the following lemma for an alternative connection.

Lemma 8.1. *Let α be a given particle velocity. Let $u^L = (s^L, \pi^L, c^L)$ and $u^B = (s^B, s^B, c^L) \in \mathcal{P}$ be such that $\lambda_{ps}^L > \lambda_p^B = \alpha$. Let $u^L = (s^L, s^B, c^L)$ be such that $h^L = h^L$. Then, $\lambda_{ps}^L < \alpha$ if and only if there exist the unique states $u^J = (s^J, s^J, c^J)$, $c^L < c^J$, and $u^L = (s^L, s^J, c^L)$, $h^L = h^L$, such that $\lambda_{ps}^L = \lambda_p^J = \alpha$.*

Proof. The necessity follows from the fact that we have three conditions for the three unknowns s^J , c^J and s^L . For sufficiency, notice that for such u^J and u^L , $\alpha = \lambda_{ps}^L > \lambda_{ps}^L$. \square

Note that if $u^I = (s^I, s^J, c^J) \in \mathcal{B}_s$ is the unique state for which $\lambda_{ps}^I = \lambda_{ps}^J$, then u^I and u^J can be connected by a bs -shock of speed λ_p^J . Afterwards, u^J can be connected to u^M by a p -wave. Hence,

the sequence

$$u^L \xrightarrow{ps} u^I \xrightarrow{bs} u^J \xrightarrow{p} u^M \quad (19)$$

is a compatible sequence that consists of a single discontinuity. For simplicity we will denote such a discontinuity by $u^L \xrightarrow{cd} u^M$. Finally, u^M and u^R can be connected by a ps -wave. As a result, we have proven the following lemma.

Lemma 8.2. *Let $u^R \in \mathcal{P}_s \cup \mathcal{T}_s$ and u^L be such that $\lambda_{ps}^F, \lambda_{ps}^L > \lambda_{ps}^R$. Let u^L, u^B and u^M be as in Figure 11. If $\lambda_{ps}^L \geq \lambda_{ps}^R$ then the solution is given by the unique compatible sequence*

$$u^L \xrightarrow{st} u^L \xrightarrow{bs} u^B \xrightarrow{p} u^M \xrightarrow{ps} u^R. \quad (20)$$

Otherwise, the solution is given by the unique sequence

$$u^L \xrightarrow{st} u^L \xrightarrow{cd} u^M \xrightarrow{ps} u^R, \quad (21)$$

where u^L is as in Lemma 8.1 and \xrightarrow{cd} is as in (19).

Note that all the waves in (21) are discontinuities that travel with speed λ_{ps}^R . Thus the connection $u^L \rightarrow u^R$ in the physical space is just one contact discontinuity. Next, to find the complete set of solutions we consider the following two cases for the left state.

Case 1: $\pi^L = \pi^R$. For such left states, there are different possibilities described in Table III. Note that in the first two solutions, all the flow is secondary with $\pi = \pi^R$. However, when $s^L > s^A$ and $\lambda_{ps}^R < \lambda_{ps}^F$, any compatible sequence will pass through some intermediate states with larger π . Solutions for such Riemann problems are given by Lemma 8.2. Note that when $s^L = s^A$ and $\lambda_{ps}^R \geq \lambda_{ps}^F$, the solution is unique in the physical space but not in the state space and is L^1 continuous with respect to the initial data but not pointwise.

Case 2: $s^L = \pi^L > \pi^R$. The different possibilities for this case are shown in Table IV. Note that when $\lambda_{ps}^R \geq \lambda_{ps}^F$, both states u^B and u^L lie on a concave segment of the flow curve and their Buckley-Leverett speeds are less than the particle velocities. Hence, both states can be connected by a primary rarefaction followed by a secondary one with final speed equal to λ_{bs}^B . Thereafter, a faster ps -wave will take over to u^R .

$s^L \leq s^A$	$\exists! u^I = (s^I, \pi^R, c^R) \in B_s$ $\exists \lambda_{ps}^I = \lambda_{ps}^L$ $u^L \xrightarrow{ps} u^I \xrightarrow{bs} u^R$		
$s^L > s^A$	$\lambda_{ps}^R \geq \lambda_{ps}^F$	$u^L \xrightarrow{bs} u^B \xrightarrow{ps} u^R$	
	$\lambda_{ps}^R < \lambda_{ps}^F$	$\lambda_{ps}^L \geq \lambda_p^B$ $u^L \xrightarrow{st} u^L \xrightarrow{bs} u^B \xrightarrow{p} u^R$ $u^I \xrightarrow{ps} u^R$	
	$\lambda_{ps}^R < \lambda_{ps}^F$	$\lambda_{ps}^L < \lambda_p^B$ $u^L \xrightarrow{st} u^I \xrightarrow{cd} u^M \xrightarrow{ps} u^R$	

TABLE III. Solutions for $c^L < c^R$, $u^R \in \mathcal{P}_s \cup \mathcal{T}_s$ and $\pi^L = \pi^R$.

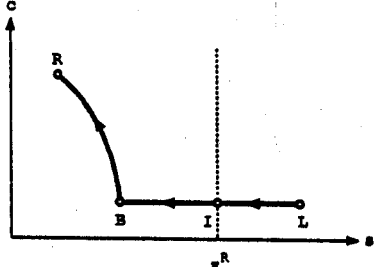
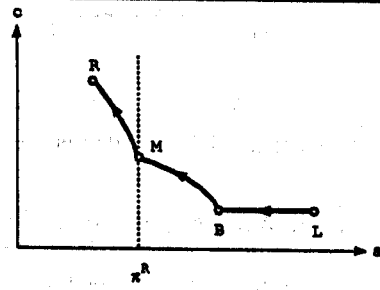
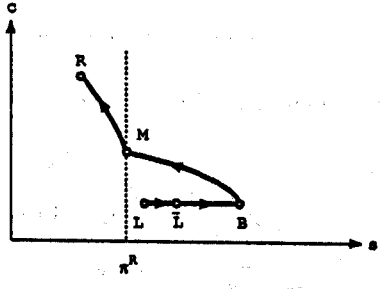
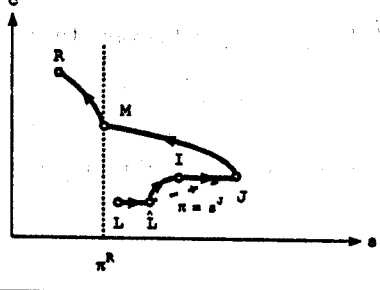
$\lambda_{ps}^R \geq \lambda_{ps}^F$	$u^I = (\pi^R, \pi^R, c^L)$ $u^L \xrightarrow{b} u^I \xrightarrow{bs} u^B \xrightarrow{ps}$ u^R		
	$s^L \geq s^B$	Let $u^I = (\pi^R, \pi^R, c^I)$, $c^L \leq c^I < c^R, \ni \lambda_p^I = \lambda_{ps}^R$ $u^L \xrightarrow{b} u^B \xrightarrow{p} u^M \xrightarrow{ps}$ u^R	
$\lambda_{ps}^R < \lambda_{ps}^F$	$s^L < s^B$	$\lambda_p^L \geq \lambda_p^B$ $u^L \xrightarrow{st} u^L \xrightarrow{bs} u^B \xrightarrow{p}$ $u^M \xrightarrow{ps} u^R$	
		$\lambda_p^L < \lambda_p^B$ $u^L \xrightarrow{st} u^L \xrightarrow{cd} u^M \xrightarrow{ps}$ u^R	

TABLE IV. Solutions for $c^L < c^R, u^R \in \mathcal{P}_s \cup \mathcal{T}_s$, and $s^L = \pi^L > \pi^R$.

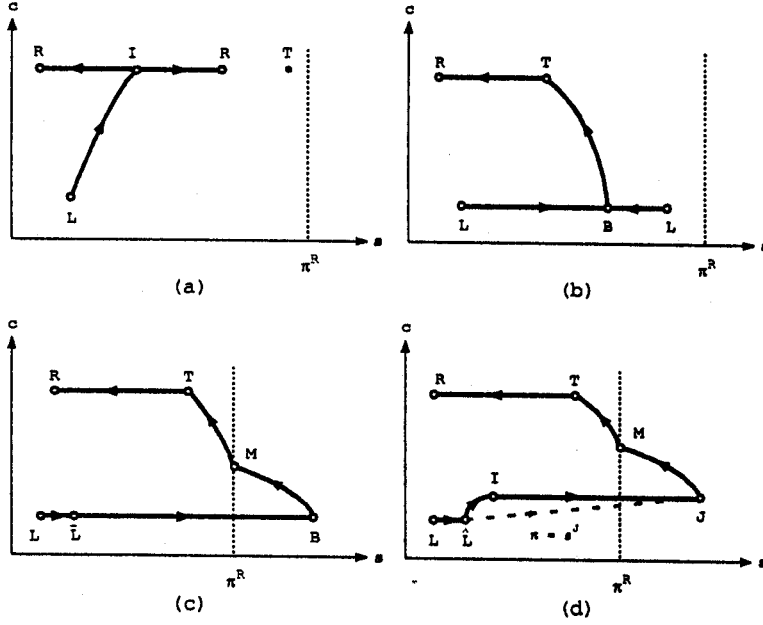


FIGURE 12. Solutions for $c^L < c^R$, $u^R \in \mathcal{B}_s$, $\pi^R \geq s^{\tan}(c^R)$ and $\pi^L = \pi^R$.

When $\lambda_{ps}^R < \lambda_{ps}^F$ we need to distinguish two possibilities for s^L with respect to s^B . First, if $s^L \geq s^B$, then u^L can be connected to u^B with a b -rarefaction of final speed equals to λ_b^B . Since $u^B \in \mathcal{P}$, any p -wave passes through u^B will be faster and thus the two waves are compatible. Second, if $s^L < s^B$, then the solutions are given by Lemma 8.2.

8.2. The Case $u^R \in \mathcal{B}_s$. Unlike in section 8.1, where $\pi^R \geq s^{\tan}(c^R)$, in this section π^R can also be less than $s^{\tan}(c^R)$. For the first case the same connections in section 8.1 can be used to connect u^L to u^T followed by a bs -wave to u^R . For the second case, we need to construct other different compatible connections.

To account for all different possibilities, we will characterize the left states according to the relation between π^R and $s^{\tan}(c^R)$, and some relating states as follows.

Case 1: $\pi^R \geq s^{\tan}(c^R)$. Let $u^T = (s^{\tan}(c^R), \pi^R, c^R)$ if it exists, otherwise let $u^T = (\pi^R, \pi^R, c^R)$.

Note that for $u^L = (s^L, \pi^R, c^L) \in \mathcal{B}_s$ such that $\lambda_{ps}^L \leq \lambda_{ps}^T$, the solution is the same as in Case 1 of section 8.1 for $s^L \leq s^A$ and shown in Figure 12a. Otherwise, u^T can be connected to u^L as in section 8.1 with u^T in place of u^R and to u^R by a bs -wave. See Figures 12 and 13 for the different solutions.

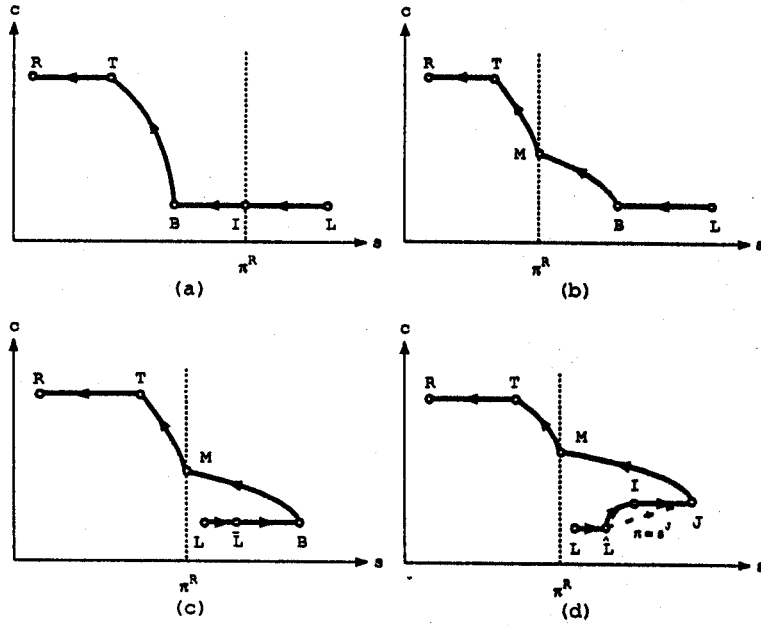


FIGURE 13. Solutions for $c^L < c^R$, $u^R \in B_s$, $\pi^R \geq s^{tan}(c^R)$ and $s^L = \pi^L > \pi^R$.

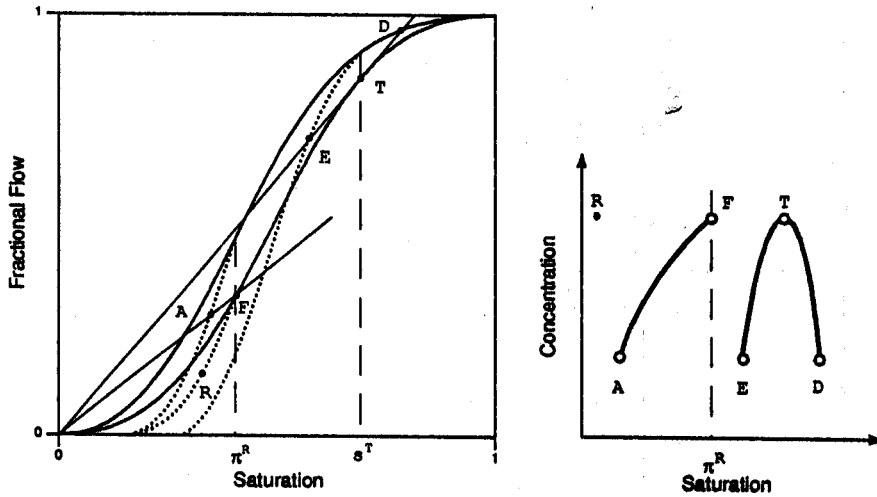


FIGURE 14. The states u^T , u^D , u^F and u^A .

Case 2: $\pi^R < s^{tan}(c^R)$. The solution will vary according to the position of u^L with respect to some states associated with $u^T = (s^T, s^T, c^R)$, $s^T = s^{tan}(c^R)$, and $u^F = (\pi^R, \pi^R, c^R)$. Let $u^A = (s^A, \pi^R, c^L)$, $u^E = (s^E, s^T, c^L)$ and $u^D = (s^D, s^D, c^L)$ be the states that satisfy $\lambda_{ps}^A = \lambda_p^F$ and $\lambda_{ps}^E = \lambda_p^D = \lambda_p^T$ as shown in Figure 14.

Considering the left states with $\pi^L = \pi^R$, we can characterize three different possibilities listed in Table V. If $h^L \leq h^A$, the solution is as in Case 1 of section 8.1 with $s^L \leq s^A$ and the flow is secondary. When $h^A < h^L \leq h^E$, a geometric inspection shows that there exists a unique pair of states $u^I = (s^I, s^I, c^R)$ and $u^L = (s^L, s^I, c^L)$ that satisfy the two conditions: $\lambda_{ps}^L = \lambda_p^I$ and

$h^L \leq h^A$	$u^L \xrightarrow{ps} u^I \xrightarrow{bs} u^R$		
$h^A < h^L \leq h^E$	$u^L \xrightarrow{st} u^{\bar{L}} \xrightarrow{ps} u^I \xrightarrow{b}$ $u^F \xrightarrow{bs} u^R$		
$h^E < h^L$	$\lambda_{ps}^L \geq h^L$	$u^L \xrightarrow{st} u^{\bar{L}} \xrightarrow{bs} u^D \xrightarrow{p}$ $u^T \xrightarrow{b} u^F \xrightarrow{bs} u^R$	
	$\lambda_{ps}^L < h^L$	$u^L \xrightarrow{st} u^{\bar{L}} \xrightarrow{cd} u^T \xrightarrow{b}$ $u^F \xrightarrow{bs} u^R$	

TABLE V. Solutions for $c^L < c^R, u^R \in B_s, \pi^R < s^{\tan(c^R)}$ and $\pi^L = \pi^R$.

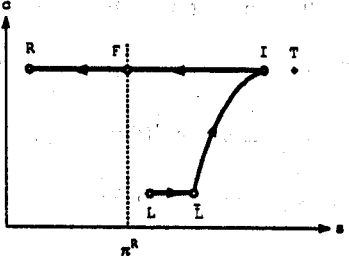
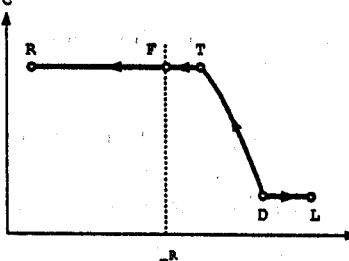
$h^L \leq h^E$	$u^L \xrightarrow{st} u^I \xrightarrow{pa} u^I \xrightarrow{b} \dots$ $u^F \xrightarrow{ba} u^R$		
$h^L > h^E$	$s^L \leq s^D$	As in Table V.
$h^L > h^E$	$s^L > s^D$	$u^L \xrightarrow{b} u^D \xrightarrow{p} u^T \xrightarrow{b} \dots$ $u^F \xrightarrow{ba} u^R$	

TABLE VI. Solutions for $c^L < c^R$, $u^R \in B_s$, $\pi^R < s^{tan}(c^R)$ and $s^L = \pi^L > \pi^R$.

$h^L = h^L$. These intermediate states are used to form the compatible sequence. Finally, when $h^E < h^L$, let $u^L = (s^L, s^D, c^L)$ be the state such that $h^L = h^L$ and the solution can be constructed as in Lemma 8.2.

Similarly, for the left states with $s^L = \pi^L > \pi^R$, the solutions will vary according to the values of h^L with respect to h^E as listed in Table VI.

SUMMARY

In this paper we studied the effect of hysteresis on the multiphase flow in porous media. We presented a model for the hysteresis in relative permeabilities and discussed the corresponding fractional flows. The model is based on considering the initial imbibition of the aqueous phase as the primary flow and any other flow as secondary. We assumed that secondary curves for imbibition and drainage are identical. We analyzed a non-strictly hyperbolic system modeling polymer flooding with hysteretic fractional flows and constructed the global solution for the corresponding Riemann problem.

Due to the hysteresis and generality of the model, it was not practical to deal with a fixed

partition of the state space. Instead, for each case we looked at a suitable criterion to account for all possibilities. Although many possibilities end up having similar solutions, we did not group them together because of their different criteria and to make the construction process easy to follow. Our purpose in presenting the different cases is to provide useful test problems for numerical methods.

Including hysteresis produced more complicated flows. This indicates that hysteresis may effect the oil recovery efficiency. In a later paper we will verify numerically the solutions above using second-order Godunov method and present the effect of hysteresis on oil recovery efficiency.

Acknowledgment. I would like to thank Prof. John Trangenstein, for his help and guidance in this research. His invaluable advice, direction and encouragement are greatly appreciated. I would also like to thank Dr. Richard Hornung for his useful comments.

REFERENCES

1. S M Buckley and M C Leverett, *Mechanisms of fluid displacement in sands*, Trans. Amer. Inst. Min. Meta. Engrs. 146 (1942), 107-116.
2. J Colonna, F Brissaud, and J L Millet, *Evolution of capillarity and relative permeability hysteresis*, SPEJ Trans. 253 (1972), 28-38.
3. Forrest F Craig, *The reservoir engineering aspects of waterflooding*, Monograph Series, Society of Petroleum Engineers, Dallas, 1971.
4. Robert E Gladfelter and Surendra P Gupta, *Effect of fractional flow hysteresis on recovery of tertiary oil*, Soc. Pet. Engrs. J. 20 (1980), 508-520.
5. Eli L Isaacson, *Global solution of a Riemann problem for a non-strictly hyperbolic system of conservation laws arising in enhanced oil recovery*, Unpublished.
6. Thormod Johansen and Rangnar Winther, *The solution of the Riemann problem for a hyperbolic system of conservation laws modeling polymer flooding*, SIAM J. Math. Anal. 19 (1988), no. 3, 541-566.
7. Barbara L Keyfitz and Herbert C Kranzer, *A system of non-strictly hyperbolic conservation laws arising in elasticity*, Arch. Rational Mech. Anal. 72 (1980), 220-241.
8. J E Killough, *Reservoir simulation with history-dependent saturation functions*, Soc. Pet. Engrs. J. 16 (1976), 37-48.
9. R J Lenhard and J C Parker, *A model for hysteretic constitutive relations governing multiphase flow, 2. permeability-saturation relations*, Water Resources Res. 23 (1987), no. 12, 2197-2206.

10. D Marchesin, H B Medeiros, and P J Paes-Leme, *A model for two phase flow with hysteresis*, Contemporary Math. 60 (1987), 89-107.
11. O A Oleinik, *Uniqueness and a stability of the generalized solution of the Cauchy problem for a quasilinear equation*, Uspekhi Mat. Nauk 14 (1959), 165-170, English translation in Amer. Math. Soc. Transl. Ser. 2, 33(1964), 285-290.
12. Gary A Pope, *The application of fractional flow theory to enhanced oil recovery*, Soc. Pet. Engrs. J. 20 (1980), 191-205.
13. John A Trangenstein and Richard B Pember, *The Riemann problem for longitudinal motion in an elastic-plastic bar*, SIAM J. Sci. Statist. Comput. 12 (1991), no. 1, 180-207.
14. H J Welge, *A simplified method for computing oil recovery by gas or water drive*, Trans. Amer. Inst. Min. Meta. Engrs. 195 (1985), 91-98.